

FAULT TOLERANT CONTROL OF A LORENTZ SELF BEARING MOTOR CONSIDERING OPEN COIL FAULTS

Lyndon Scott Stephens, Associate Professor

Anand Ranganathan, Research Assistant

University of Kentucky, Bearings and Seals Laboratory

Department of Mechanical Engineering

151 Ralph G. Anderson Building, Lexington, KY 40506-0503

Phone: (859) 257-6336, Fax: (859) 257-3304, E-mail: stephens@engr.uky.edu

ABSTRACT

This paper presents a decoupling and fault tolerant control algorithm for a segmented arc, Lorentz self bearing motor with open coil faults. The particular motor uses 12 phases to produce forces in the x and y directions and the motoring torque. The algorithm uses the redundancy in these phases to adapt to open coil faults that result in failed phases. In this approach a model of the actuator torque-current and force-current relationship is computed for a given fault condition. Since this model includes the commutation sequence for the motor, it must be computed at each sampled time step. This model is then inverted onto itself which reduces the current gain matrix to the identity matrix and eliminates any cross-coupling effects. Any desired current gain matrix is then achieved by inserting it into the feed forward path. Results indicate a high level of redundancy in the actuator such that several faults can be accommodated simultaneously. The results also show that the cost of a fault may be a higher power usage and lower peak force/torque ability.

INTRODUCTION

The slotless, segmented arc, Lorentz self bearing motor was first analyzed by Stephens and Kim [1,2]. Its advantages include no trade-off between actuator force and motoring torque with permanent magnet thickness, ultra-smooth angular slewing due reduced cogging torque and precise angular pointing. The most significant disadvantage of this design is that the actuator current gain and negative stiffness matrices were found to be cross-coupled and to vary with the rotor angle. The approach taken has been to treat this cross-coupling and variation as model uncertainty and to synthesize robustly stable controllers. The robustness of such controllers was evaluated using μ -

analysis while treating the uncertainties as structured [3]. That work demonstrated the successful stabilization of the motor for all rotor angles. However, a subsequent analysis [4] showed that the high level of uncertainty limits the bearing stiffness and reduces the stable region hence impacting performance, as one would expect from uncertainty. These effects emphasize the importance of decoupling the model to provide a stable bearing force and motoring torque with improved performance.

Open coil actuator faults in magnetic actuators result in a change in both the magnitude and direction of the actuator force. This is essentially a cross-coupling of the actuator. Therefore, decoupling control and fault tolerant control of an actuator can be addressed as one and the same. Fault tolerant control of magnetic actuators can be addressed by redundant hardware and/or adaptive control software. Stephens and Kim analyzed different coil winding schemes to minimize the impact of an open coil fault on the Lorentz self bearing motor [5]. Meecker [6] developed a general mathematical basis to address fault tolerant control in Maxwell type actuators. Several additional schemes have been proposed for achieving reliable electromagnetic devices including controller board approaches that make use of re-bias linearization. Na and Palazzolo developed an optimization technique, which made the magnetic bearing fault tolerant to many pole and coil failures [7].

In this paper, the approach to fault tolerant and decoupling control for the Lorentz self bearing motor utilizes the redundancy in the 12 motor phases to generate only 2 radial bearing forces and 1 motoring torque. The model inversion approach is shown to result in complete decoupling and stable control in spite of multiple open coil failures.

MOTOR DESCRIPTION

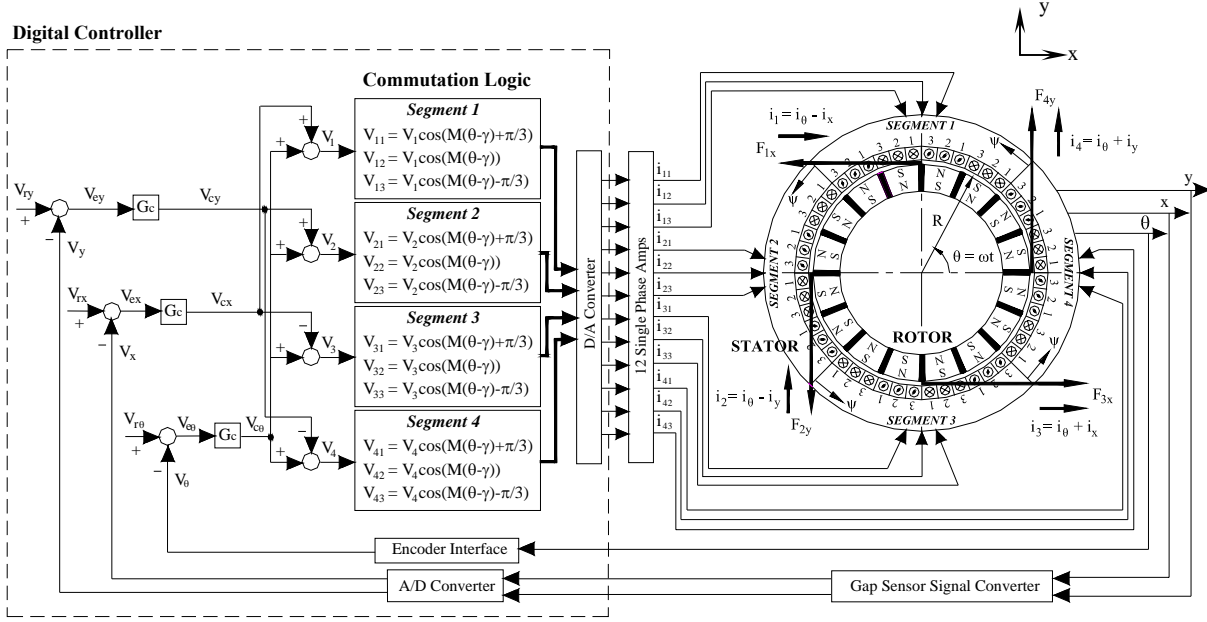


Figure 1: Lorentz Self Bearing Motor and Control System Under No Fault

Figure 1 shows the layout of the slotless Lorentz self bearing motor along with the feedback control system for the case of no coil faults. The actuator consists of $M=8$ permanent magnet pole pairs attached to the rotor and $N=4$ individually controlled winding segments attached to the stator. Each winding segment in the motor is an arc of $\pi/2$ radians and is attached to the slotless back iron. The windings occupy $N_s=12$ stations along each winding segment ID with $N_w=85$ individual wires per station. The 12 stations are divided into 4 sets of 3 phase windings. Each segment generates a traction on the surface of the rotor due to the PM flux linking with the segment windings (a Lorentz-type force). By precise construction of the motor, the tractions due to segments 1-4 are resolved into the forces F_{1x} , F_{2y} , F_{3x} and F_{4y} . Decoupled PID controllers, $G_{cx}(s)$, $G_{cy}(s)$ and $G_{c\theta}(s)$ are used to generate the control voltages V_{cx} , V_{cy} and $V_{c\theta}$. By proper mapping of the control voltages to each segment, the segment forces are modulated to produce bearing forces in the x and y directions and motoring torque in the θ direction. In the no fault condition the mapping is the sum and difference of the control voltages as shown in the figure resulting in the segment voltages, V_1 , V_2 , V_3 and V_4 . This mapping essentially provides an x direction bearing force by decreasing the force F_{1x} and increasing the force F_{3x} . The y direction force is generated in a like manner by decreasing the force F_{2y} and increasing the force, F_{4y} . Each of the segment control voltages are distributed into 3 phases

per segment per the commutation logic as shown in the figure. This results in the 12 phase voltages, $V_{11}-V_{43}$. Twelve transconductance power amplifiers are finally used to generate the corresponding 12 phase currents, $\mathbf{i}_\phi = [i_{11} \ i_{12} \ i_{13} \ \dots \ i_{44}]^T$ where i_{11} is the current in segment 1, phase 1 and so forth. For the purposes of this development the amplifier gains are assumed to be unity therefore system voltages and currents are used interchangeably. For this system the force-current relationship for the motor was found to be [1]:

$$\begin{bmatrix} F_x \\ F_y \\ T_\theta \end{bmatrix} \approx \underbrace{\begin{bmatrix} K_{xx}(\theta) & [K_{xy,w}\bar{i}_\theta \pm K_{ly}(\theta)] & K_{xy}\bar{i}_y \\ -[K_{xy,w}\bar{i}_\theta \pm K_{ly}(\theta)] & K_{xx}(\theta) & K_{xy}\bar{i}_x \\ 0 & 0 & K_\theta \end{bmatrix}}_{[K_i]} \begin{bmatrix} i_x \\ i_y \\ i_\theta \end{bmatrix} + \underbrace{\begin{bmatrix} K_{xx,M} + K_{xx,w} & K_{xy,L}\bar{i}_\theta & 0 \\ -K_{xy,L}\bar{i}_\theta & K_{xx,M} + K_{xx,w} & 0 \\ 0 & 0 & 0 \end{bmatrix}}_{[K_d]} \begin{bmatrix} x \\ y \\ \theta \end{bmatrix} \quad (1)$$

where $[K_i]$ is the current gain matrix, $[K_d]$ is the negative stiffness matrix, \mathbf{z} is the displacement vector, \mathbf{i}_c is the vector of control currents and \mathbf{F}_c is the vector of

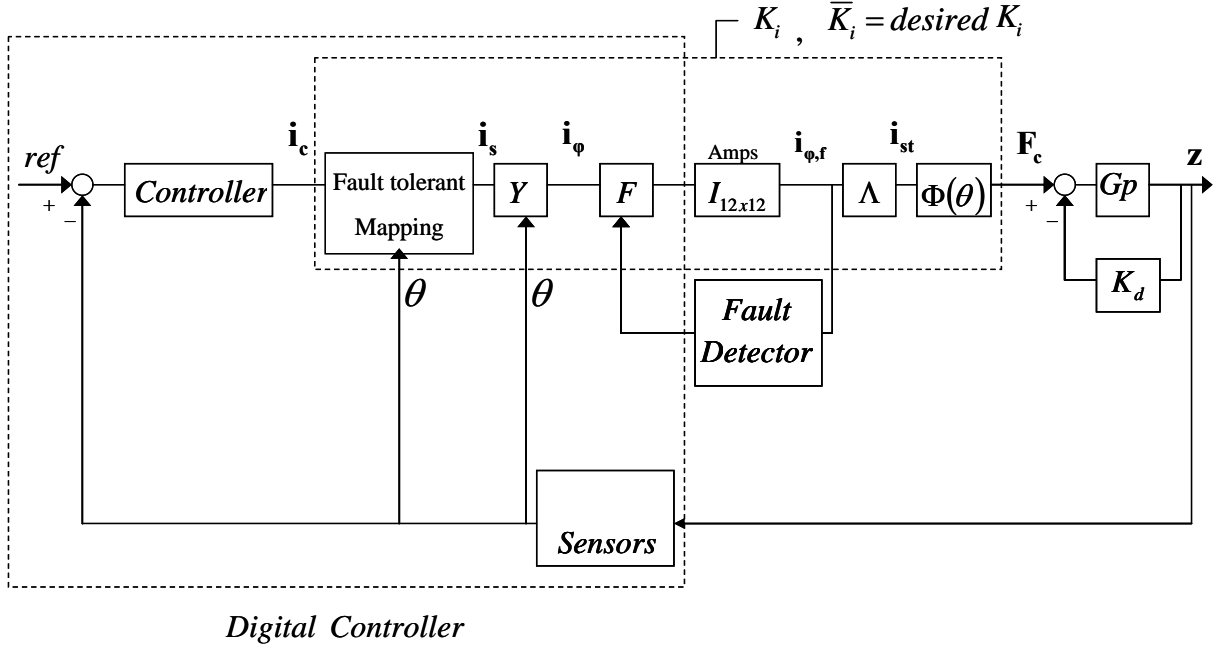


Figure 2: Fault Tolerant and Decoupling Control Approach

control forces. Note that the current gain matrix is cross-coupled and that the direct terms are also a function of the rotor angle, θ . In previous work the magnitudes of these cross-couplings and variations were shown to be sufficiently small such that stable levitation is achievable by treating them as plant uncertainty. However, note that if a fault occurs in a given phase then the magnitude and direction of the segment forces will not be resolved exactly into the x and y directions. Therefore, the current gain matrix will become even more cross-coupled. The fundamental basis of this paper is that all open coil faults essentially result in various degrees of cross-coupling of the current gain matrix. Therefore, the fault tolerant control problem is one of identifying and decoupling the current gain matrix for each rotor angle.

FAULT TOLERANT CONTROL APPROACH

Fault tolerant control is achieved by constructing a detailed model of the force-current relationship at each rotor angle, θ , and simply inverting that model onto itself to decouple the system. Referring to Figure 2, the inverted model is inserted in the “fault tolerant mapping” block. The appropriate mapping depends upon the relationship between the actuator force vector, F_c , and the actuator segment current vector, i_s , which is given by:

$$\begin{bmatrix} F_{cx} \\ F_{cy} \\ T_{c\theta} \end{bmatrix} = \underbrace{\begin{bmatrix} 3 \times 48 \\ \Phi(\theta) \end{bmatrix}}_A \underbrace{\begin{bmatrix} 48 \times 12 \\ \Lambda \end{bmatrix}}_A \underbrace{\begin{bmatrix} 12 \times 12 \\ F \end{bmatrix}}_A \underbrace{\begin{bmatrix} 12 \times 4 \\ Y(\theta) \end{bmatrix}}_A \begin{bmatrix} i_1 \\ i_2 \\ i_3 \\ i_4 \end{bmatrix} \quad (2)$$

In this equation, $Y(\theta)$ is the *commutation matrix* that distributes the 4 segment currents into the 12 phase currents, $i_{\phi} = Y i_s$, and is constructed as:

$$Y = \begin{bmatrix} \phi_1 & 0 & 0 & 0 \\ \phi_2 & 0 & 0 & 0 \\ \phi_3 & 0 & 0 & 0 \\ 0 & \phi_1 & 0 & 0 \\ 0 & \phi_2 & 0 & 0 \\ 0 & \phi_3 & 0 & 0 \\ 0 & 0 & \phi_1 & 0 \\ 0 & 0 & \phi_2 & 0 \\ 0 & 0 & \phi_3 & 0 \\ 0 & 0 & 0 & \phi_1 \\ 0 & 0 & 0 & \phi_2 \\ 0 & 0 & 0 & \phi_3 \end{bmatrix}$$

$$\begin{aligned} \phi_1 &= \cos[m(\theta - \gamma) + \pi/3] \\ \phi_2 &= \cos[m(\theta - \gamma)] \\ \phi_3 &= \cos[m(\theta - \gamma) - \pi/3] \end{aligned} \quad (3)$$

F is the *fault matrix* and is a 12x12 identity matrix for the case of the no fault condition. A zero is put on the diagonal in place of a one to indicate a fault, such that $i_{\phi,f} = F i_{\phi}$, where $i_{\phi,f}$ is the vector of phase currents including zeros currents for the phases that have failed.

The matrix Λ is termed the *phase distribution matrix* and describes how the phase currents are distributed around the stator inner diameter and is dependent upon the particular winding pattern used for the coils. Referring again to Figure 1, for this actuator there are 4 three phase winding stations (12 total) per segment for a total of 48 segments. Thus the winding station current vector is computed by $i_{st} = \Lambda i_{\phi,f}$, where:

$$\mathbf{i}_{st} = \begin{bmatrix} i_{1(1)} & i_{1(2)} & i_{1(3)} & i_{1(4)} & \dots & i_{4(11)} & i_{4(12)} \end{bmatrix}^T \quad (4)$$

and where $i_{1(2)}$ is the current in segment 1 at winding station number 2 and so forth. Note that the winding stations in Figure 1 are numbered in the counterclockwise direction. The phase distribution matrix therefore consists of block diagonal matrices given by:

$$\Lambda = \begin{bmatrix} \beta_{2 \times 3} & 0 & 0 & 0 \\ 0 & \beta_{2 \times 3} & 0 & 0 \\ 0 & 0 & \beta_{2 \times 3} & 0 \\ 0 & 0 & 0 & \beta_{2 \times 3} \end{bmatrix} \quad (5)$$

where $\beta_{12 \times 3}$ consists of identity matrices of the form:

$$\beta_{2 \times 3} = \begin{bmatrix} -I_{3 \times 3} \\ I_{3 \times 3} \\ -I_{3 \times 3} \\ I_{3 \times 3} \end{bmatrix} \quad (6)$$

Note that a negative sign indicates that the station currents are going into the page in Figure 1 (when the rotor is in the home position as shown) and a positive sign indicates that the station currents are coming out of the page.

Finally, the matrix Φ is the *flux linkage matrix* that relates the individual station currents to the actuator forces as $\mathbf{F}_c = \Phi \mathbf{i}_{st}$. This matrix depends upon the orientation of each winding station with respect to the x, y and θ direction, and on the permanent magnet flux distribution. For the j^{th} winding station the orientation with respect to the x axis is:

$$\psi_j = \frac{\pi}{4} + \frac{\pi}{N_{st}} + (j-1) \frac{2\pi}{N_{st}} \quad (7)$$

where N_{st} is the total number of winding stations. For the j^{th} winding station the permanent magnet flux density is computed using a sinusoidal approximation as:

$$B_j = B_m \sin(M(\theta - \psi_j)) \quad (8)$$

where B_m is the flux density magnitude. The flux linkage matrix is therefore:

$$\Phi = N_w L \begin{bmatrix} -B_1(\theta) \sin \psi_1 & B_1(\theta) \cos \psi_1 & RB_1(\theta) \\ -B_2(\theta) \sin \psi_2 & B_2(\theta) \cos \psi_2 & RB_2(\theta) \\ \vdots & \vdots & \vdots \\ -B_{48}(\theta) \sin \psi_{48} & B_{48}(\theta) \cos \psi_{48} & RB_{48}(\theta) \end{bmatrix}^T \quad (9)$$

where R is the rotor outer radius, N_w is the number winding turns per station and L is the stator axial length. Note that the model, $A = \Phi \Lambda F Y$, maps the 4 segment currents to the 3 control forces for a given fault condition and is, in general, cross coupled. The model is completely decoupled by defining the fault tolerant mapping between the segment currents and the control currents as:

$$\mathbf{i}_s = A^+ \bar{K}_i \mathbf{i}_c \quad (10)$$

where $A^+ = A^T(AA^T)^{-1}$ and is the Moore-Penrose pseudo inverse of the underdetermined model, A, and \bar{K}_i is any *desired current gain matrix* as defined by the designer. Of course the desired current gain matrix is of the completely decoupled variety and may be as simple as the identity matrix. Combining equations (2) and (10) illustrates how the method essentially cancels the original system, whether it has a fault or not, and replaces it with the desired current gain matrix:

$$\mathbf{F}_c = \frac{AA^+}{I} \bar{K}_i \mathbf{i}_c \quad (11)$$

Note that this mapping solves the problem of cross-coupling and current gain variation that exists in this actuator even for the case of no fault, as well as provides a current gain matrix that remains invariant under open coil faults.

SIMULATED RESULTS

For the purposes of analysis an actuator geometry consistent with an existing experimental test rig is considered. The actuator considered has $N_w=85$ windings per station, an outer rotor radius of $R=50.8$ mm, an axial length of $L=25.4$ mm, and a peak PM flux density of $B_m=0.77$ T. In previous work the nominal direct current gains for this actuator were found to be $K_{ixx}=K_{iyy}=18.26$ N/A and $K_{i\theta}=2.05$ N-m/A. Therefore, the desired decoupled current gain matrix under any fault condition is taken as:

$$\bar{K}_i = \begin{bmatrix} 18.26 & 0 & 0 \\ 0 & 18.26 & 0 \\ 0 & 0 & 2.05 \end{bmatrix} \quad (12)$$

The results presented below are for this sample actuator.

A. MAXIMUM NUMBER OF COIL FAULTS

A central question is: Under what combination of open coil faults does the actuator still perform? The analogous question is: For what values of the fault matrix, F, does A^+ exist for all rotor angles, θ ? Since

$A^+ = A^T(AA^T)^{-1}$, then existence depends on $(AA^T)^{-1}$, which does not exist when AA^T is singular. Therefore, for a given fault condition, F , the actuator can still

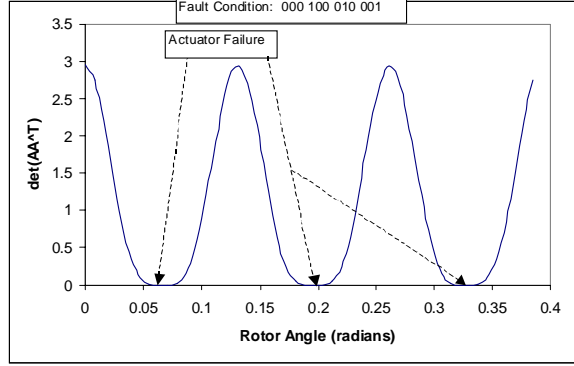


Figure 3: Typical Fault Evaluation Plot

perform as long as:

$$|AA^T| \neq 0 \quad \forall \theta \quad (12)$$

Figure 3 illustrates this computation for a fault condition of $\text{diag}(F)=[000 \ 100 \ 010 \ 001]$ which indicates faults in all phases of segment 1, phases 2 and 3 of segment 2, phases 1 and 3 of segment 3 and phases 1 and 2 of segment 4. Note that $|AA^T|=0$ at three rotor angles per pole pitch indicating that the actuator cannot perform under this combination of faults and is therefore unstable. This fault evaluation was performed for a variety of possible faults for this actuator. Table 1 below summarizes the results. From this table it is seen that due to the high level of redundancy in the actuator (12 phases used to generate 2 forces and 1 torque), it is able to perform under a large number of possible open coil faults.

Table 1: Fault Condition Evaluation

Description	Seg 1	Seg 2	Seg 3	Seg 4	Result
	1 2 3	1 2 3	1 2 3	1 2 3	
No Faults	1 1 1	1 1 1	1 1 1	1 1 1	Stable
All phases in one segment failed	0 0 0	1 1 1	1 1 1	1 1 1	Stable
All segments with phase 2 failed	1 0 1	1 0 1	1 0 1	1 0 1	Stable
All segments with phase 1 failed (same as phase 3)	0 1 1	0 1 1	0 1 1	0 1 1	Stable
All phases in 1 segment plus 1 phase in adjacent segment	0 0 0	1 0 1	1 1 1	1 1 1	Stable
All phases in 1 segment plus 1 phase in opposite segment	0 0 0	1 1 1	1 0 1	1 1 1	Stable
All phases in 2 opposite segments	0 0 0	1 1 1	0 0 0	1 1 1	Unstable
All phases in 2 adjacent segments	0 0 0	0 0 0	1 1 1	1 1 1	Unstable
All phases in 1 segment and 2 in opposite segment	0 0 0	1 1 1	0 1 0	1 1 1	Unstable
All phases in 1 segment and 1 in opposite segment	0 0 0	1 1 1	1 1 0	1 1 1	Stable
All phases in 1 segment and 1 in adjacent segment	0 0 0	1 0 1	1 1 1	1 1 1	Stable
2 different phases failed in each segment	0 0 1	0 1 0	1 0 0	0 0 1	Unstable

B. DECOUPLING & FAULT INVARIANCE

Table 2: Decoupling and Fault Invariance for Control Current Vector $i_c = [1 \ 1 \ 1]^T$

Fault Cond.	Rotor Angle	Variable	\bar{K}_i (Desired)	No Fault Tolerant Control	Fault Tolerant Control
111 111 111 111	$\theta=0^\circ$	Fxx (N)	18.26	18.26	18.26
		Fyy (N)	18.26	18.26	18.26
		T (N-m)	2.05	2.05	2.05
111 111 111 111	$\theta=2.81^\circ$	Fxx (N)	18.26	17.27	18.26
		Fyy (N)	18.26	19.22	18.26
		T (N-m)	2.05	2.05	2.05
000 100 010 001	$\theta=0^\circ$	Fxx (N)	18.26	2.63	18.26
		Fyy (N)	18.26	2.63	18.26
		T (N-m)	2.05	0.3422	2.05
000 100 010 001	$\theta=2.81^\circ$	Fxx (N)	18.26	-0.797	18.26
		Fyy (N)	18.26	7.591	18.26
		T (N-m)	2.05	0.4424	2.05

Table 2 shows the results of two simulations as compared to the desired decoupled current gain matrix. One simulation is based on the original control of the system with no fault tolerance or decoupling. The other simulation is based on the fault tolerant control algorithm. This table gives the resulting actuator forces in the x, y and θ directions when the control currents are 1 ampere for each axis. The first fault condition examined is $\text{diag}(F)=[111 \ 111 \ 111 \ 111]$ which corresponds to no fault. Since the actuator gains are known to vary with rotor angle, results are presented for the home position of $\theta=0^\circ$ and for $1/2$ of a pole pitch or $\theta=2.81^\circ$ in this actuator. The effectiveness of the algorithm is seen in decoupling the actuator over all rotor angles for this fault condition. The second fault condition examined is $\text{diag}(F)=[000 \ 100 \ 010 \ 001]$ which corresponds to a condition where only 3 phases are operational in the actuator. The effectiveness of the algorithm in handling a large number of open coil faults is seen as for this condition as the system is clearly unstable when no fault tolerant control is used.

C. PERFORMANCE DEGRADATION

The preceding results show that the fault tolerant control algorithm clearly results in an invariant current gain matrix under many fault combinations. The natural question is then: What price is paid for these faults? There are two:

- 1) The total current draw and hence the actuator power loss increases, all else being equal.
- 2) For a given peak current limit, the maximum force and torque generation decreases, all else being equal.

Figure 4 shows the peak force and torque capacity for a given fault condition assuming that the maximum RMS current in a given coil is limited to 2 amperes. (In a Lorentz force actuator this limit is a function of thermal dissipation. As coils fail, this limit may be increased. However, for the purposes of illustration it is assumed that this is a fixed limit.) This figure clearly demonstrates the reduction in peak force and torque capacity that occurs as the number of faults increases.

Figure 5 illustrates how the total current used by the actuator to produce a given set of bearing forces and torque is increased as more faults occur. In this figure the control current vector is maintained at $i_c = [0.5 \ 0 \ 0.5]^T$. As a fault occurs, the algorithm will adjust the phase currents to maintain the desired bearing force and torque. As the figure shows, in general, the total current used by all phases tends to increase as the number of faults increases. Note that for a specific rotor angle, this may not always be the case, but for a given fault condition over all rotor angles, the total

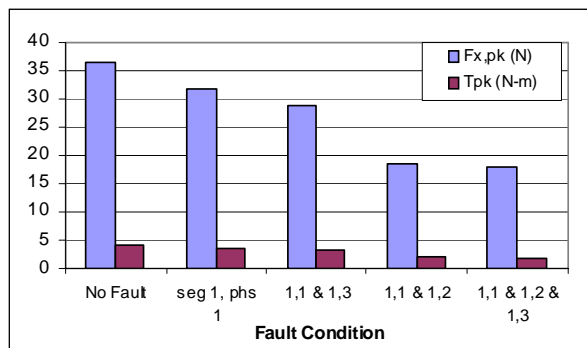


Figure 4: Peak Force and Torque Capacity for a Given Fault Condition

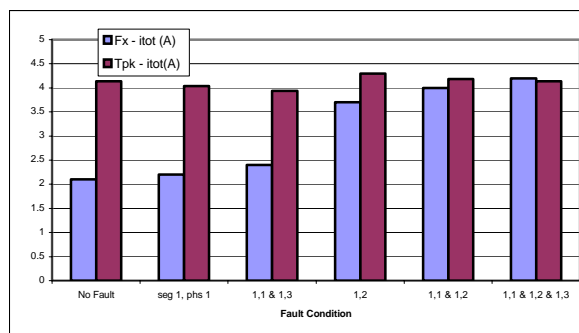


Figure 5: Total Current to Achieve Desired Force and Torque for a Given Fault Condition

current draw will always increase, hence reducing the efficiency of the motor. This fault tolerant algorithm therefore provides a graceful degradation in performance of the actuator.

CONCLUSIONS

The model based algorithm presented in this paper has the potential to decouple the segmented arc, Lorentz self bearing motor and to provide graceful degradation in performance under open coil faults. The analysis showed a high level of fault protection under the algorithm which is due to the redundancy in the actuator. The cost of the fault protection was found to be a lower limit on peak actuator force and torque, and a high power loss. Future work will focus on experimental results and on the robustness of the algorithm to uncertainty in the model.

REFERENCES

1. Stephens, L.S. and Kim, D.G., "Analysis and Simulation of A Lorentz-Type, Slotless Self Bearing Motor", *Control Engineering Practice*, 10, (2002) pp. 899-905
2. Stephens, L.S. and Kim, D.G., "Force and Torque Characteristics for a Slotless, Lorentz Self Bearing Servomotor", *IEEE Transactions on Magnetics*, Vol. 38, No. 4, July 2002
3. Stephens, L.S., and Chin, H.M., "Robust Stability of the Lorentz Type Self Bearing Servomotor", *Proceedings of the 8th International Symposium on Magnetic Bearings*, Mito, Japan, August 2002
4. Chin, H.M., *Controller Design Issues and Performance of the Lorentz Self Bearing Motor*, Masters Thesis, University of Kentucky, December, 2003
5. Kim, D.G. and Stephens, L.S., "Fault Tolerance of a Lorentz-Type Slotless, Self Bearing Motor According to Coiling Schemes", *Proc. Of the 7th Int'l Symp. On Magnetic Bearings*, Zurich, August, 2000
6. Meeker, D.C., "Optimal Solutions to Inverse Problems in Quadratic Magnetic Actuators", Doctoral Dissertation, University of Virginia, May, 1996
7. Na, U.J. and Palazzola, A.B., "Optimized realization of Fault tolerant Heteropolar Magnetic Bearing for Active vibration Control", *Proceedings of the ASME Design Engineering Conference*, September, 1999